precursor-ion scanning, in which marker ions such as *m/z* 204 ($HexNAc^+$) produced from glycoproteins by collision-induced decomposition (CID) are monitored, can trace only glycopeptides in proteolytic-digested glycoproteins.

The present chapter describes the following methods:

1. Proteolytic digestion of a glycoprotein.
2. LC–MS analysis of a proteolytic-digested glycoprotein.
   a. Peptide/glycopeptide mapping.
   b. Glycopeptide mapping.
3. LC–MS/MS analysis of a proteolytic-digested glycoprotein.

Using EPO as an example of a glycoprotein, we also present here applications of LC–MS and LC–MS/MS with glycoproteins.

2. Materials

2.1. Proteolytic Digestion of Glycoproteins

1. Proteases. Choose a protease or proteases that will cleave the glycoprotein into glycopeptides containing one glycosylation site. Enzyme specificity is as follows:
   a. Trypsin: Lys/Arg-↓-X,
   b. Endoproteinase Lys-C (Lys-C): Lys-↓-X,
   c. Endoproteinase Glu-C (Glu-C): Glu(Asp)-↓-X,
   d. Endoproteinase Asp-N (Asp-N): X-↓-Asp(Glu)
2. Protease solution (*see* **Note 1**):
   a. Trypsin: Dissolve TPCK-trypsin (Sigma, St. Louis, MO) in 3 m*M* HCl at a final concentration of 2 μg/μL.
   b. Lys-C: Dissolve Lys-C (Roche Diagnostics, GmbH, Germany) in 100 m*M* ammonium acetate, pH 8.6, at a final concentration of 0.4 μg/μL.
   c. Glu-C: Dissolve Glu-C (Roche Diagnostics, GmbH, Germany) in 100 m*M* ammonium acetate, pH 8.0, at a final concentration of 4 μg/μL.
   d. Asp-N: Dissolve Asp-N (Wako Pure Chemical Industries, Ltd., Osaka, Japan) in 25 m*M* ammonium bicarbonate, pH 8.0, at a final concentration of 0.1 μg/μL.
3. Proteolytic digestion buffer:
   a. Trypsin: 100 m*M* Tris-HCl, pH 8.0.
   b. Lys-C: 100 m*M* ammonium acetate, pH 8.6.
   c. Glu-C: 100 m*M* ammonium acetate, pH 8.0.
   d. Asp-N: 25 m*M* ammonium bicarbonate, pH 8.0.
4. Reduction and carboxymethylation buffer: 0.5 *M* Tris-HCl (pH 8.6) containing 8 *M* guanidine hydrochloride and 5 m*M* EDTA.
5. 2-Mercaptoethanol.
6. Monoiodoacetic acid.
7. Sephadex G-25 column, e.g., PD-10 column (Amersham Biosciences, Uppsala, Sweden).

2.2. LC–MS and LC–MS/MS Analyses of Proteolytic-Digested Glycoproteins

LC–MS/MS analysis (Precursor-ion scanning) generally requires a larger amount of sample than LC–MS analysis (normal scanning). Use of a microbore column (1.0 mm id) is, therefore, recommended for precursor-ion scanning.

1. HPLC equipment:
   a. For LC–MS: A gradient pump equipped with an injector, a column oven, an integrator, and a detector capable of monitoring UV absorbance at 206 nm.
   b. For LC–MS/MS: A gradient pump equipped with an injector, an integrator, and a UV monitor equipped with a microflow cell (0.3 μL), e.g., Magic 2002 (Michrom BioResources, Inc. Auburn, CA).
2. ESI-MS and -MS/MS: Triple-stage quadrupole mass spectrometer equipped with an electrospray ion source, e.g., Finnigan TSQ-7000 (Thermo Finnigan, Inc. San Jose, CA).
3. Column:
   a. For LC–MS: Vydac 218TP52 (250 × 2.1 mm, Vydac, Hesperia, CA), and Pegasil ODS (250 × 2.1 mm, Senshu Science Co. Ltd., Tokyo, Japan).
   b. For LC–MS/MS: Magic C18 (150 × 1.0 mm, Michrom BioResource, Inc. Auburn, CA).
4. HPLC mobile phase (*see* **Note 2**):
   a. For peptide/glycopeptide mapping by LC/MS:
      Solvent A: 0.05% TFA.
      Solvent B: 0.05% TFA/50 %(v/v) acetonitrile.
   b. For glycopeptide mapping by LC–MS:
      Solvent A: 1 m*M* ammonium acetate, pH 6.8.
      Solvent B: 1 m*M* ammonium acetate, pH 6.8/80% (v/v) acetonitrile.
   c. For precursor-ion scanning by LC–MS/MS:
      Solvent A: 0.05% TFA/2%(v/v) acetonitrile.
      Solvent B: 0.05% TFA/80%(v/v) acetonitrile.

3. Methods

3.1. Proteolytic Digestion of Glycoproteins

Glycoproteins that possess multiple disulfide bonds are reduced and derivatized with monoiodoacetic acid for the complete proteolysis as follows (**steps 1–4**). These steps can be omitted for glycoproteins having only a few disulfide bonds.

1. Dissolve a glycoprotein (360 μg) in 360 μL of reduction and carboxymethylation buffer.
2. Add 2.6 μL of 2-mercaptethanol, and incubate the mixture at room temperature for 2 h.
3. To the reaction mixture, add 7.56 mg of monoiodoacetic acid and incubate the mixture at room temperature for 2 h in the dark.

4. Apply the reaction mixture on a Sephadex G-25 column to remove the reagents, and lyophilize the effluent (*see* **Note 3**).
5. Dissolve the glycoprotein in proteolytic digestion buffer to a final concentration of 1 mg/mL.
6. Add protease solution, and incubate the sample at 37°C for 1–24 h.
   a. Trypsin: Add trypsin solution to a final protein:enzyme ratio of 50:1, and incubate for 1–4 h (*see* **Note 4**).
   b. Lys-C: Add Lys-C solution to a final protein:enzyme ratio of 25:1, and incubate for 24 h.
   c. Glu-C: Add Glu-C solution to a final protein:enzyme ratio of 50:1, and incubate for 20 h (*see* **Note 5**).
   d. Asp-N: Add Asp-N solution to a final protein:enzyme ratio of 50:1, and incubate for 20 h.
7. Store the sample at –20°C before use.

Erythropoietin contains three *N*-glycans at Asn 24, 38, and 83, and one *O*-glycan at Ser-126 ***(6)***. This glycoprotein has two disulfide bonds (*see* **Fig. 1**). The structures of *N*-glycans in EPO are reported to be fucosylated bi-, tri-, and tetraantennary oligosaccharides containing 0–4 sialic acid with 0–3 *N*-acetyllactosamine (*see* **Fig. 2**) ***(3,7–9)***. Glu-C solution (62 µL) was added to EPO (1 mg) dissolved in 1 mL of 100 m*M* ammonium acetate, pH 8.0, and the sample was incubated at 37°C for 20 h. EPO is expected to be digested into four glycopeptides, E5, E6, E10, and E12, and some peptides, as shown in **Fig. 1**.

3.2. LC–MS Analysis of a Proteolytic-Digested Glycoprotein

3.2.1. Peptide/Glycopeptide Mapping

1. Equilibrate a column with the starting solvent (1% of B) at a flow rate of 0.2 mL/min, and monitor the absorbance at 206 nm. Set the column oven to 40°C.
2. Set the ESI voltage and electron multiplier to 4500V and 1200V, respectively. Set the capillary temperature to 225°C. Adjust the pressure of the sheath gas (N_2) and auxiliary gas (N_2) to 70 psi and 10 U, respectively. Set the scan time to 4 s. Perform ionization and acquire the ions at *m/z* 550–2400 in the positive ion mode (*see* **Note 6**).
3. Inject an aliquot (50 µL) of the sample onto the HPLC column.
4. Elute the column using a linear gradient from 1% to 90% of B in 130 min at a flow rate of 0.2 mL/min.

An elution profile of Glu-C-digested EPO is shown in **Fig. 3**. Amino acid residues in nonglycosylated peptides were determined by comparing the experimental masses with the masses predicted from the cDNA-derived amino acid sequence (*see* **Fig. 1**). Mass spectra of glycopeptides E5, E6, E10, and E12 are present in **Fig. 4**. Carbohydrate structures and amino acid residues of the ions

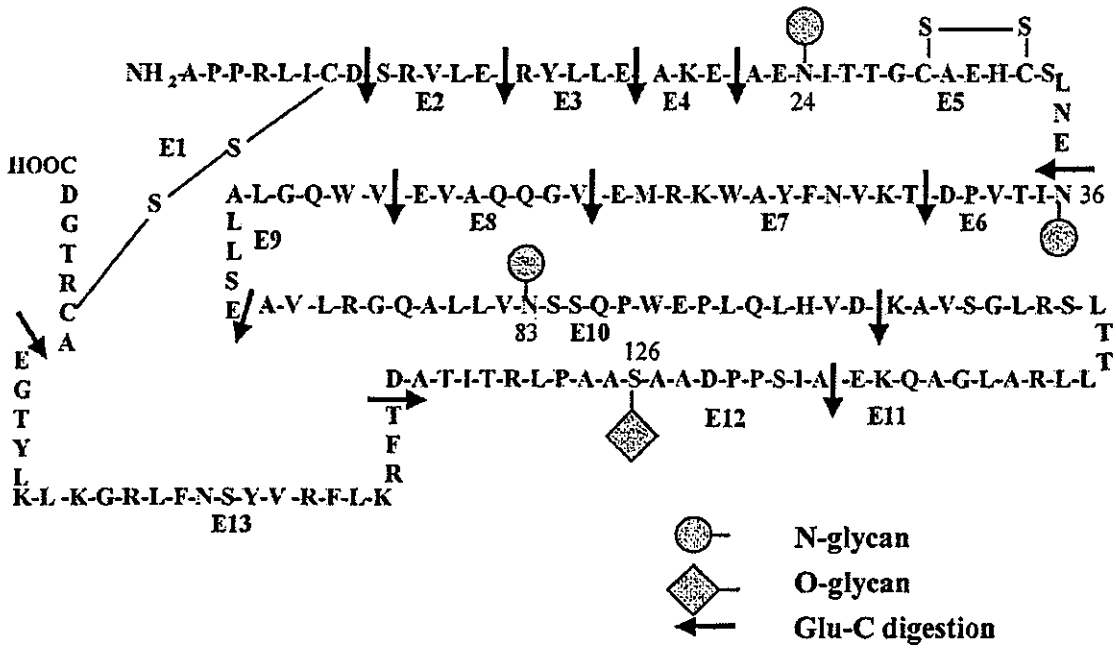

Fig. 1. Amino acid sequence and glycosylation sites of erythropoietin.

mental and theoretical masses of peptides and carbohydrates (*see* **Fig. 2**). The structural assignment of peaks shown in **Fig. 3** is summarized in **Table 1**.

3.2.2. Glycopeptide Mapping

1. Equilibrate a column with the starting solvent (1% of B) at a flow rate of 0.2 mL/min, and monitor the absorbance at 206 nm. Set the column oven to 40°C.
2. Set the ESI voltage, electron multiplier, and capillary temperature to 4500V, 1200V, and 225°C, respectively. Adjust the pressure of the sheath gas (N_2) and auxiliary gas (N_2) to 70 psi and 10 U, respectively. Set the scan time to 3 s. Perform ionization and acquire the ions at *m/z* 1000–2400 in the positive ion mode (*see* **Note 7**).
3. Apply the sample (15 µL) on the HPLC column.
4. Elute the column using a linear gradient from 1% to 6% of B in 60 min followed by a further increase of solvent B up to 36% within 80 min (*see* **Note 8**).

The glycopeptide map of Glu-C-digested EPO is shown in **Fig. 5A**. Four glycopeptides were eluted in the order of E6 (Asn36), E5 (Asn24), E12 (Ser126), and E10 (Asn83), and the glycopeptides were further separated based on the structure of the oligosaccharides attached to each glycosylation site. For example, glycopeptide E6 was separated into 10 peaks (*see* **Fig. 5B**). These glycoforms were eluted in the order of tetra-, tri-, and disialylated glycopeptides, and they were further separated based on the number of *N*-acetyllactosamine

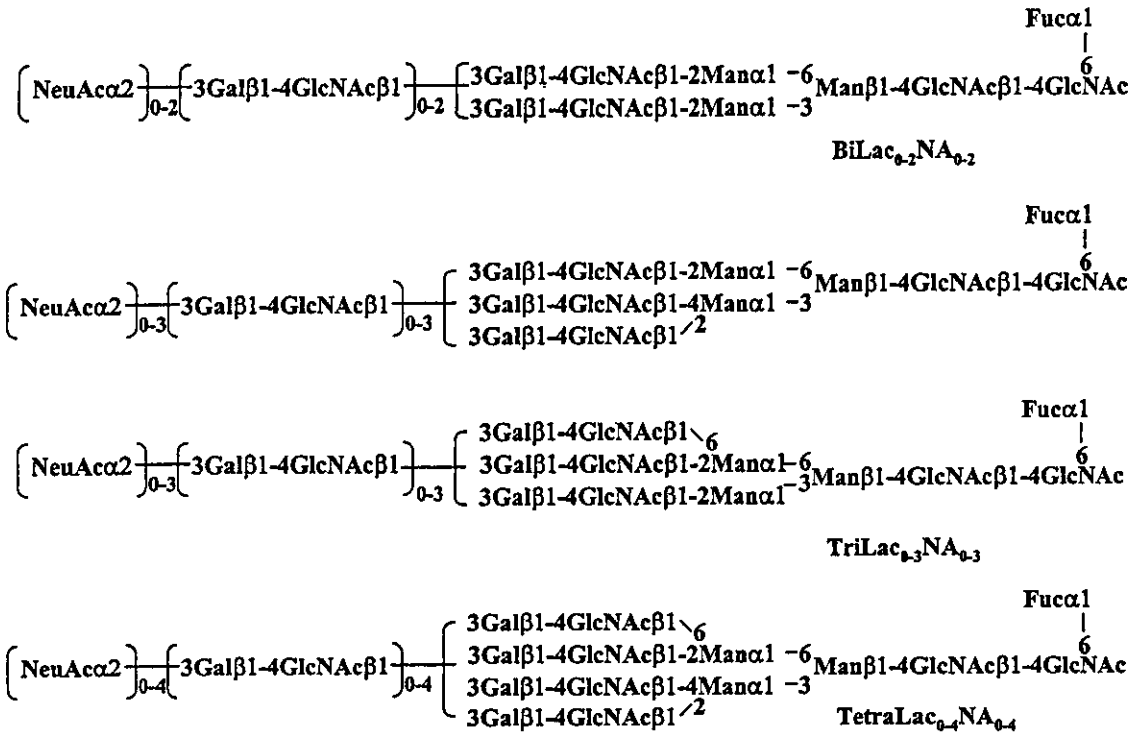

Fig. 2. Carbohydrate structures of erythropoietin. Bi, biantennary; Tri, triantennary; Tetra, tetraantennary; Lac, *N*-acetyllactosamin; NA, NeuAc.

3.3. LC–MS/MS Analysis of a Proteolytic-Digested Glycoprotein

1. Equilibrate a microbore column (1.0 mm id) with the starting solvent (5% of B) at a flow rate of 50 µL/min, and monitor the absorbance at 206 nm.
2. Set the ESI voltage and the electron multiplier to 4500v and 1500 V, respectively. Set the capillary temperature to 225°C. Adjust the pressure of the sheath gas (N_2) and auxiliary gas (N_2) to 70 psi and 10 U, respectively. Set the collision energy and pressure of the collision gas (Ar) to –20 eV and 2.0 mTorr, respectively. Set the scan time to 4 s. Perform ionization in the positive ion mode and acquire the ions at *m/z* 400–2400 with the first quadrupole (Ql), and at *m/z* 204 with the third quadrupole (Q3) in the precursor-ion scan mode (*see* **Note 9**).
3. Inject an aliquot (8 µL) of the sample onto the HPLC column.
4. Elute the column using a linear gradient from 5 to 45% of B in 40 min at a flow rate of 50 µL/min.

Figure 6 shows the TIC chromatograms of Glu-C digested EPO, which was obtained by normal scan (LC–MS) (**A**) and by the precursor-ion scan of *m/z* 204 ($HexNAc^+$) (LC–MS/MS) (**B**). Nonglycosylated peptides are eliminated by the precursor-ion scan, resulting in a TIC chromatogram showing only glycopeptides *(10)*.

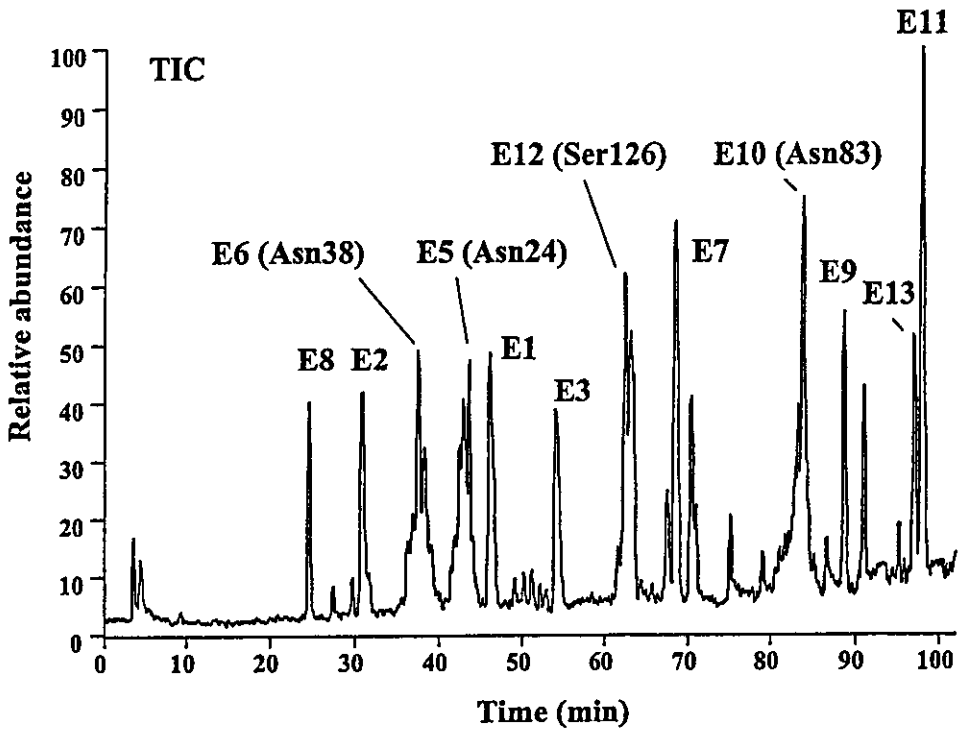

Fig. 3. Glu-C peptide/glycopeptide map of erythropoietin. Column, Vydac 218TP52 (250 × 2.1 mm); eluent A, 0.05% TFA; eluent B, 0.05% TFA/50% (v/v) acetonitrile; gradient, 1 to 90% of B in 130 min; flow rate, 0.2 mL/min; acquired mass, *m/z* 550–2400; ion mode, negative; sample amount, 50 µg erythropoietin.

4. Notes

1. The protease solution can be stored at –20°C for 1 yr.
2. To reduce background, the use of Milli-Q filtrated water is recommended. The mobile phase should be prepared just before use.
3. Instead of Sephadex-G25, reverse-phased (RP) HPLC may be used for desalting; recovery of some glycoproteins, however, is decreased by the derivatization and removal of the denaturant.
4. Peaks that cannot be identified sometimes appear as a result of excess incubation with trypsin. It is worth checking the reaction after 1 h of incubation.
5. Glu-C digests Glu-X without cleavage of Asp-X at a 1:50 enzyme-to-substrate ratio at pH 8.0. Asp-X can be hydrolyzed by Glu-C at a 1:4 enzyme-to-substrate ratio.
6. The positive ion mode is recommended for analyses of peptides and nonsialylated glycoproteins. The negative ion mode is effective for analyses of sialylated glycopeptides.
7. The range of *m/z* 1000–2400 is effective for selective detection of glycopeptides. Most of the nonglycosylated peptides can be eliminated in this range.

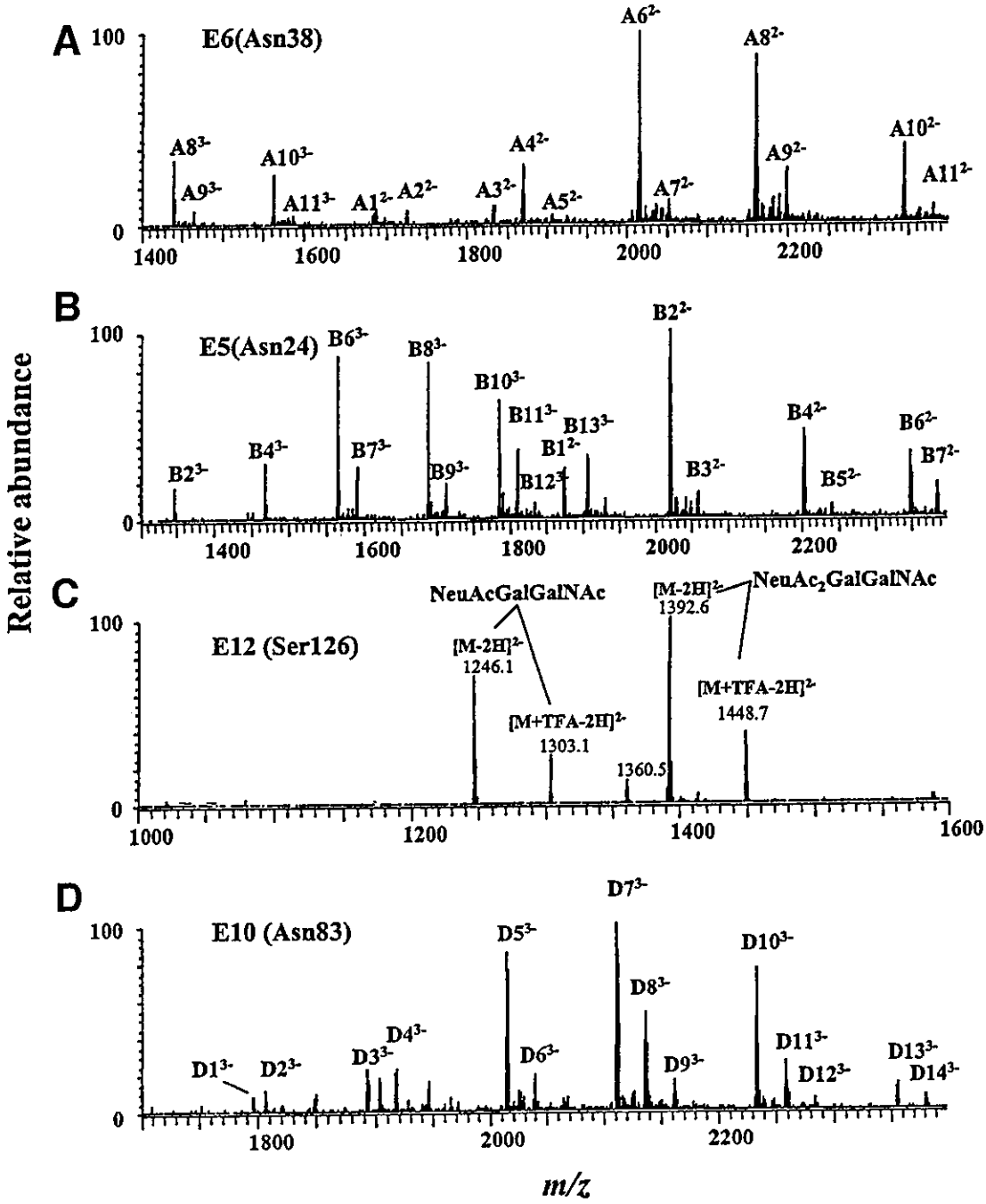

Fig. 4. Mass spectra of glycopeptides E6 (A), E5 (B), E12 (C), and E10 (D). Peak assignment is presented in **Table 1**.

8. Since some nonglycosylated peptides are not eluted by ammonium acetate, it is recommended to wash the column with 0.05%TFA/80% acetonitrile for 15 min after the analysis.

Table 1
Structural Assignments of Peaks in Fig. 3 and of Ions in Fig. 4, and Their Theoretical Masses and Observed *m/z* Values

Peptide in Fig. 3	Amino acid residues	Ion in Fig. 4	Carbohydrate structure[a]	Theoretical mass[b]	Observed *m/z*		
					M^-	M^{2-}	M^{3-}
E8	56–62			729.8	728.4		
E2	9–13			602.7	601.5		
E6	38–43	A1	$BiLac_1NA_2$, $TriNA_2$[c]	3375.2		1686.8	
		A2	$TriLac_1NA_1$, $TetraNA_1$[d]	3449.3		1724.4	
		A3	$TriNA_3$	3666.5		1831.8	
		A4	$BiLac_2NA_2$, $TriLac_1NA_2$, $TetraNA_2$[e]	3740.6		1869.1	
		A5	$TriLac_2NA_1$, $TetraLac_1NA_1$[f]	3814.6		1906.5	
		A6	$TriLac_1NA_3$, $TetraNA_3$[g]	4031.8		2014.5	
		A7	$TriLac_2NA_2$, $TetraLac_1NA_2$[h]	4105.9		2052.8	
		A8	$TetraNA_4$	4323.1		2160.2	1440.1
		A9	$TriLac_2NA_3$, $TetraLac_1NA_3$[i]	4397.1		2198.0	1465.1
		A10	$TetraLac_1NA_4$	4688.4		2343.2	1561.8
		A11	$TetraLac_2NA_3$	4762.5		2380.2	1586.5
E5	22–37	B1	$BiNA_1$	3750.7		1875.1	
		B2	$BiNA_2$	4042.0		2020.3	1346.2
		B3	$TriNA_1$	4116.0		2058.5	
		B4	$BiLac_1NA_2$, $TriNA_2$[c]	4407.3		2202.7	1468.2
		B5	$TriLac_1NA_1$, $TetraNA_1$[d]	4481.4		2239.8	
		B6	$TriNA_3$	4698.6		2348.7	1565.6
		B7	$BiLac_2NA_2$, $TriLac_1NA_2$, $TetraNA_2$[e]	4772.6		2385.7	1590.7
		B8	$TriLac_1NA_3$, $TetraNA_3$[g]	5063.9			1687.3
		B9	$TriLac_2NA_2$, $TetraLac_1NA_2$[h]	5138.0			1712.2
		B10	$TetraNA_4$	5355.2			1784.5
		B11	$TriLac_2NA_3$, $TetraLac_1NA_3$[i]	5429.2			1809.6
		B12	$TetraLac_2NA_2$	5503.3			1834.0
		B13	$TetraLac_1NA_4$	5720.5			1905.7
E1	(1–8)S-S (160–165)			1503.7	1502.1	750.6	
E3	14–18			692.8	691.5		
E12	118–136		NA-Gal-GalNAc	2494.6		1246.1	
			NA_2-Gal-GalNAc	2785.9		1392.6	
E7	45–55			1572.9	1571.1		
E10	73–96	D1	$BiLac_1NA_2$, $TriNA_2$[c]	5388.5			1795.1
		D2	$TriLac_1NA_1$, $TetraNA_1$[d]	5462.6			1820.5
		D3	$TriNA_3$	5679.8			1892.2
		D4	$BiLac_2NA_2$, $TriLac_1NA_2$, $TetraNA_2$[e]	5753.9			1917.6
		D5	$TriLac_1NA_3$, $TetraNA_3$[g]	6045.1			2014.2
		D6	$TriLac_2NA_2$, $TetraLac_2NA_2$[h]	6119.2			2040.0
		D7	$TetraNA_4$	6336.4			2111.1
		D8	$TriLac_2NA_3$, $TetraLac_1NA_3$[i]	6410.5			2136.4
		D9	$TetraLac_2NA_2$	6484.6			2161.6
		D10	$TetraLac_1NA_4$	6701.7			2233.4
		D11	$TetraLac_2NA_3$	6775.8			2258.2

(continued)

Table 1 *(continued)*

Peptide in Fig. 3	Amino acid residues	Ion in Fig. 4	Carbohydrate structure[a]	Theoretical mass[b]	Observed *m/z* M^-	M^{2-}	M^{3-}
		D12	$TetraLac_3NA_2$	6849.9			2283.5
		D13	$TetraLac_2NA_4$	7067.1			2355.8
		D14	$TetraLac_3NA_3$	7141.1			2380.8
E9	63–72			1115.3	1113.9		
E13	137–159			2837.4		1418.4	
E11	97–117			2212.6	2211.4		

[a]All N-glycans contain fucosylated core. Bi, biantennary; Tri, triantennary; Tetra, tetraantennary; NA, NeuAc; Lac, *N*-acetyllactosamine.

[b]Average mass value.

[c–i]Isomers.

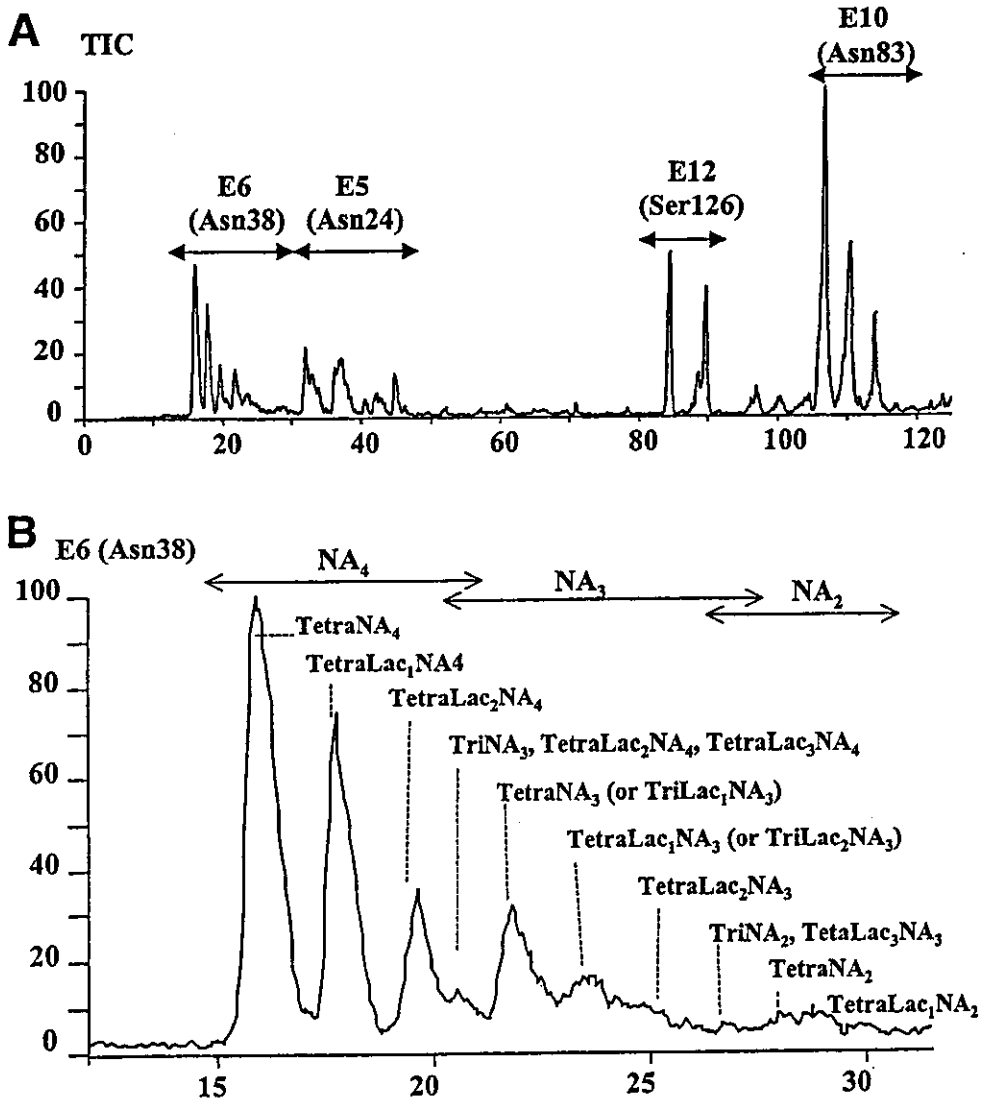

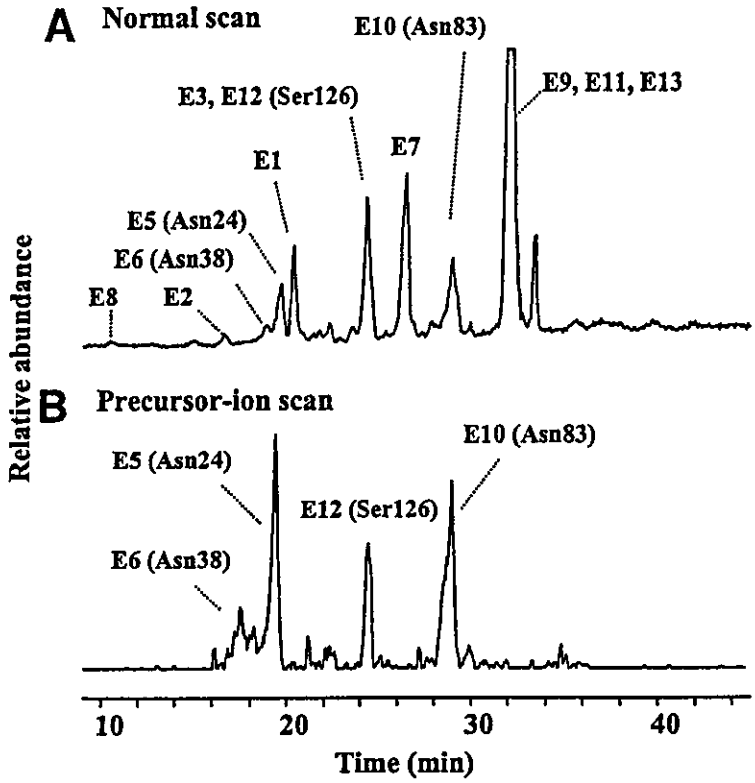

Fig. 6. Normal scan (A) and precursor-ion scan (B) of Glu-C-digested EPO. Column, Magic C18 (150 × 1 mm); eluent A, 0.05%TFA/2% acetonitrile; eluent B, 0.05% TFA/80% acetonitrile; gradient, 5 to 45% of B in 40 min; flow rate, 50 µL/min; acquired mass (Q1), *m/z* 400–2400. Set mass (Q3), *m/z* 204; ion mode, positive; sample amount, 2 µg (A) and 8 µg (B) of erythropoietin.

9. Monitoring of the oxonium ions *m/z* 204 ($HexNAc^+$) and 366 ($Hex\text{-}HexNAc^+$) is effective for the determination of both *N*-glycosylated and *O*-glycosylated peptides.

References

1. Hayakawa, T. (1991) in *Drug Biotechnology Regulation. Scientific Basis and Practices* (Chiu, Y.-Y. H. and Gueriguian, J. L., eds.), Marcel Dekker, New York, pp. 468–498.

Fig. 5. *(see opposite page)* (A) Glu-C glycopeptide map of erythropoietin. Column, Vydac 218TP52 (250 × 2.1 mm); eluent A, 1 m*M* ammonium acetate, pH 6.8. eluent B, 1 m*M* ammonium acetate, pH 6.8/80% (v/v) acetonitrile; gradient, 1 to 6% of B in 60 min followed by 36% of B in 80 min; flow rate, 0.2 mL/min; acquired mass, *m/z* 1000–2400; ion mode, negative; sample amount, 15 µg erythropoietin. (B) Expanded view of glycopeptide E6. Bi, biantennary; Tri, triantennary; Tetra, tetraantennary; Lac,

2. Hirayama, K., Yuji, R., Yamada, N., Kato, K., Arata, Y., and Shimada, I. (1998) Complete and rapid peptide and glycopeptide mapping of mouse monoclonal antibody by LC/MS/MS using ion trap mass spectrometry. *Anal. Chem.* **70,** 2718–2725.
3. Kawasaki, N., Ohta, M., Hyuga, S., Hyuga, M., and Hayakawa, T. (2000) Application of liquid chromatography/mass spectrometry and liquid chromatography with tandem mass spectrometry to the analysis of the site-specific carbohydrate heterogeneity in erythropoietin. *Anal. Biochem.* **285,** 82–91.
4. Ohta, M., Kawasaki, N., Hyuga, S., Hyuga, M., and Hayakawa, T. (2001) Selective glycopeptide mapping of erythropoietin by on-line high-performance liquid chromatography/electrospray ionization mass spectrometry. *J. Chromatogr. A* **910,** 1–11.
5. Huddleston, M. J., Bean, M. F., and Carr, S. A. (1993) Collisional fragmentation of glycopeptides by electrospray ionization LC/MS and LC/MS/MS: Methods for selective detection of glycopeptides in protein digests. *Anal. Chem.* **65,** 877–884.
6. Krantz, S. B. (1991) Erythropoietin. *Blood* **77,** 419–434.
7. Sasaki, H., Bothner, B., Dell, A., and Fukuda, M. (1987) Carbohydrate structure of erythropoietin expressed in Chinese hamster ovary cells by a human erythropoietin cDNA. *J. Biol. Chem.* **262,** 12,059–12,076.
8. Takeuchi, M., Takasaki, S., Miyazaki, H., et al. (1988) Comparative study of the asparagine-linked sugar chains of human erythropoietins purified from urine and the culture medium of recombinant Chinese hamster ovary cells. *J. Biol. Chem.* **263,** 3657–3663.
9. Tsuda, E., Goto, M., Murakami, A., et al. (1988) Comparative structural study of N-linked oligosaccharides of urinary and recombinant erythropoietins. *Biochemistry* **27,** 5646–5654.
10. Itoh, S., Kawasaki, N., Ohta, M., Hyuga, M., Hyuga, S., and Hayakawa, T. (2001) Study on evaluating methods for the quality control of glycoprotein products. (III) Erythropoietin products. Part 3. *Kokuritsu Iyakuhin Shokuhin Eisei Kenkyusho Hokoku* **119,** 65–69.

JOURNAL OF CELLULAR PHYSIOLOGY 195:119–129 (2003)

CD31 (PECAM-1)-Bright Cells Derived From AC133-Positive Cells in Human Peripheral Blood as Endothelial-Precursor Cells

TOSHIE KANAYASU-TOYODA,[1] TERUHIDE YAMAGUCHI,[1]* TADASHI OSHIZAWA,[1] AND TAKAO HAYAKAWA[2]

[1]*Division of Cellular and Gene Therapy Products, National Institute of Health Sciences, Tokyo, Japan*

[2]*National Institute of Health Sciences, Tokyo, Japan*

To clarify the process of endothelial differentiation, we isolated AC133$^+$ cells and induced the in vitro differentiation of these cells into endothelial cells. AC133$^+$ cells efficiently differentiated into endothelial cells when the cells were cultured on fibronectin-coated dishes in the presence of vascular endothelial growth factor. Time-course analysis of the alteration of endothelial markers on cultured AC133$^+$ cells revealed that the expression of CD31 (PECAM-1) on AC133$^+$ cells was the earliest marker among all of the tested markers. Based on the hypothesis that CD31 is an early indicator during the endothelial differentiation, we examined the relationship between CD31 expression and the ability to differentiate into endothelial cells in cells derived from AC133$^+$ cells. CD31-bright cells, which were sorted from cultured AC133$^+$ cells, differentiated more efficiently into endothelial cells than had CD31-positive or CD31-negative cells, suggesting that CD31-bright cells may be precursor cells for endothelial cells. In the present study, we identified CD31$^+$ cells derived from cultured AC133$^+$ cells that are able to differentiate to endothelial cells as precursor cells. J. Cell. Physiol. 195: 119–129, 2003. © 2003 Wiley-Liss, Inc.

Recent biotechnology advances provide a new approach to an innovative therapeutics that utilizes in vitro-processing cell/tissue, so-called cell therapy (Boheler and Fiszman, 1999; Bordignon et al., 1999; Efrat, 2001; Lindvall and Hagell, 2001). The breakthrough of cell therapy might depend on the recent progress in stem cell biology, such as the induction and control of stem cells to differentiate various functional cells/tissues (Asahara et al., 2000). In particular, the committed stem and progenitor cells have recently been isolated from various adult tissues, including hematopoietic stem cells (Ziegler and Kanz, 1998; Ziegler et al., 1999), neural stem cells (Flax et al., 1998), and mesenchymal stem cells (Prockop, 1997).

Endothelial progenitor cells recently in adult blood are considered to be one of the candidates available for therapeutic neovascularization (Kalka et al., 2000) in cardiovascular diseases or hind limb ischemia diseases which may not be cured merely by the function of activated, fully differentiated endothelial cells at the site. The concept of neovascularization (vasculogenesis plus angiogenesis) in adult tissues has recently been established. Angiogenesis is defined as the development of new blood vessels from pre-existing vasculatures as induced by fully differentiated endothelial progenitor cells. Since the existence of endothelial progenitor cells derived from bone marrow has been demonstrated in adult peripheral blood, post-natal vasculogenesis has been considered to be involved in the pathological and physiological neovascularization of adult tissues (Asahara et al., 1999).

Nieda et al. (1997) reported that endothelial cell precursors, CD34$^+$ cells, are normal components of human umbilical cord blood. Circulating CD34-positive endothelial progenitor cells were isolated from adult peripheral blood. These cells were shown to differentiate into the cell lineage with endothelial cell-markers in vitro (Asahara et al., 1997; Kalka et al., 2000; Gaugler et al., 2001). Very recently, AC133$^+$ cells in circulating human peripheral blood were also identified as a population of functional endothelial progenitor cells (Peichev et al., 2000; Gill et al., 2001). The CD34$^+$ or AC133$^+$

Abbreviations: VEGF, vascular endothelial growth factor; FN, fibronectin; BSA, bovine serum albumin; PBS, phosphate buffered saline; FITC, fluorescein isothiocyanate; PE, phycoerythrin.

*Correspondence to: Teruhide Yamaguchi, Division of Cellular and Gene Therapy Products, National Institute of Health Sciences, Kamiyoga 1-18-1, Setagayaku, Tokyo 158-8501, Japan. E-mail: yamaguch@nihs.go.jp

Received 24 July 2002; Accepted 14 November 2002

Published online in Wiley InterScience (www.interscience.wiley.com), 7 February 2003.
DOI: 10.1002/jcp.10229

characteristics of endothelial progenitor cells, however, are also defined as the typical surface marker of blood stem cells (Yin et al., 1997; de Wynter et al., 1998; Punzel and Ho, 2001). Therefore, the administration of $CD34^+$ or $AC133^+$ cells into an ischemic region is thought to be an injection of endothelial progenitor cells and blood stem cells.

In the present study, we isolated $AC133^+$ cells and examined their endothelial differentiation in vitro. CD31(PECAM-1)-positive and -bright cells appeared at an early stage of the in vitro differentiation of $AC133^+$ cells, and CD31-bright cells derived from $AC133^+$ cells were identified as the precursors of endothelial cells. We discussed the significance of CD31-bright cells on the differentiation of endothelial cells.

MATERIALS AND METHODS

Reagents

Recombinant human vascular endothelial growth factor (VEGF) was purchased from Biotrend Chemikalien GmbH (Köln, Germany). The AC133-magnetic cell sorting kit was from Miltenyi Biotec (Gladbach, Germany). Anti-CD31 monoclonal antibody (BD PharMingen, San Diego, CA), anti-vonWillebrand Factor VIII monoclonal antibody (BD PharMingen), 1,1'dioctadecyl- 3,3,3',3'-tetramethylindo-carbocyanine perchlorate acetylated low density lipoprotein (DiI-Ac-LDL, Biomedical Technologies, Inc., Stoughton, MA), anti-CD34 monoclonal antibody (Nichirei, Tokyo, Japan), anti-KDR monoclonal antibody, anti-Tie2 rabbit polyclonal antibody (Santa Cruz Biotechnology, Inc., Santa Cruz, CA), anti-CD11b monoclonal antibody (BD PharMingen), and anti-human endothelial NO synthase rabbit polyclonal antibody (Cayman Chemical, MI) were obtained. Fluorescein isothiocyanate (FITC)-conjugated anti-CD34 monoclonal antibody was from BD PharMingen, and phycoerythrin (PE)-conjugated anti-AC133 monoclonal antibody was from Miltenyi Biotec. Fibronectin-, collagen type I-, and type IV-coated dishes were purchased from Iwaki Co., Japan.

Preparation of peripheral blood mononuclear cells

Buffy-coat fraction was prepared from voluntary donated human blood. The collected buffy coat was diluted with phosphate buffered saline (PBS) containing 2 mM EDTA, and was loaded on Ficoll-Paque PLUS (Amersham Pharmacia Biotech, Uppsala, Sweden) (density = 1.077). After being centrifugated for 15 min 450*g* at 15°C, mononuclear cells were collected and washed with sorting solution (PBS supplemented with 2 mM EDTA and 0.5% bovine serum albumin (BSA)).

Flowcytometric analysis of AC133 and CD34 expression in mononuclear cells

Mononuclear cells were labeled with PE-conjugated anti-AC133 monoclonal antibody and FITC-conjugated anti-CD34 monoclonal antibody simultaneously. After washing with the sorting solution, flowcytometric analysis was performed with a FACS Calibur (Becton-Dickenson, Bedford, MA).

Magnetic cell sorting of $AC133^+$ and $CD34^+$ cells

Mononuclear cells were labeled with magnetic bead-conjugated anti-$AC133^+$ antibodies according to the protocol directed by the manufacturer. In the case of $CD34^+$ cells, mononuclear cells were labeled with anti-CD34 monoclonal antibody, and then were subsequently incubated with magnetic bead-conjugated goat anti-mouse IgG antibody (Miltenyi Biotec). After the brief wash with the sorting solution, the cells were treated by a magnetic cell-separator (autoMACS, Miltenyi Biotec), and then the positive cells were collected and washed with the sorting solution.

Culture of $AC133^+$ and $CD34^+$ cells

$AC133^+$ cells and $CD34^+$ cells were cultured in EBM-2 (Clonetics, Palo Alto, CA) medium containing 20% heat-inactivated FBS, 30 mg/L kanamycin sulfate at 37°C under moisturized air containing 5% CO_2 with 50 ng/ml VEGF. Both cells were plated on fibronectin(FN)-, type IV collagen-, or type I-collagen-coated dishes at the cell density of 10^5 cells/ml. Half of the medium was exchanged once every 3–4 days with fresh medium. Periodically cells were fixed with ethanol chilled to −20°C, then subsequently subjected to an immunostaining procedure or other treatments.

Immunostaining of adherent cells

After fixation with chilled ethanol (−20°C), the cell layer was washed with PBS three times. Cells were incubated with each first antibody in 1% BSA in Tris-buffered saline (TBS; 20 mM Tris, pH 7.6, 150 mM NaCl) for 1 h at 4°C. After washing with PBS, the cells were incubated with fluorescein isothiocyanate (FITC)-conjugated anti-mouse IgG antibody or anti-rabbit IgG antibody or Rhodamin-conjugated anti-rabbit IgG antibody for 1 h at 4°C. Cells were washed with PBS and then examined using a Zeiss LSM 510 microscope with an extinction wavelength of 488 nm and an emission of 530/30 nm for FITC or 570/30 nm for Rhodamin.

In every experiment, we used non-specific immunoglobulin corresponding to the first antibody species as a control and confirmed that the cells were not stained with control immunoglobulin. The fluorescence intensity of randomly selected 20 cells was calculated using the Scion Image Program within the linear range for quantitation.

Flowcytometric analysis of CD31 expression and cell sorting

The expressions of CD31 on cultured $AC133^+$ cells were flowcytometrically determined. After $AC133^+$ cells were cultured for several days on either FN-coated or collagen type IV-coated dishes, both adherent and non-adherent cells were collected. The collected cells were labeled with FITC-labeled anti-CD31 antibody for 15 min at 4°C. After a brief wash with 0.5% BSA in PBS, flow cytometric analysis was performed. CD31-bright, CD31-positive and negative cells were sorted from cultured $AC133^+$ cells with Vantage SE (Becton-Dickenson).

Uptake of acetyl-LDL

To assess the ability of attached cells to take up acetyl-LDL, 10 μg/ml DiI acetyl-LDL was added to the medium after washing the cell layer. Cells were subsequently incubated for 30 min at 37°C. After washing three times with PBS, the cells were examined using a Zeiss (Oberkochen, Germany) LSM 510 microscope.

Statistical analysis

Statistical analysis was performed using the unpaired Student's *t*-test. Values of $P < 0.05$ were considered to indicate statistical significance. Each experiment was repeated three times and the representative data were indicated.

RESULTS

It has been reported that endothelial cells are derived from endothelial mitosis but are also differentiated from CD34-positive ($CD34^+$) cells or AC133-positive ($AC133^+$) cells as an endothelial progenitor cell (Asahara et al., 1997; Nieda et al., 1997; Kalka et al., 2000; Peichev et al., 2000; Gaugler et al., 2001; Gill et al., 2001). Since blood stem cells also express CD34 and AC133 antigen on their surface (Yin et al., 1997; de Wynter et al., 1998; Punzel and Ho, 2001), $CD34^+$ cells and $AC133^+$ cells are characterized as both blood stem cells and endothelial progenitor cells. First, we analyzed the expression of AC133 and CD34 in mononuclear cells (Fig. 1a). Yin et al. (1997) suggested that $AC133^+$ cells were a subset of $CD34^+$ cells. As shown in Figure 1a, not only $AC133^+$ $CD34^+$ cells but also $AC133^+$ $CD34^-$ and $AC133^-$ $CD34^+$ cells were observed. $AC133^+$ cells represented only 28.6% of $CD34^+$ cells. To compare the ability of $CD34^+$ cells and $AC133^+$ cells to differentiate into endothelial cells, we sorted $CD34^+$ cells and $AC133^+$ cells from peripheral blood mononuclear cells and cultured these cells on FN-coated dishes in the presence of VEGF for 2 weeks. As shown in Figure 1b, many more adherent cells were produced from $AC133^+$ cells than from $CD34^+$ cells. In order to clarify whether the adherent cells are endothelial cells, the incorporation of acetyl LDL as a function of endothelial cells (Voyta et al., 1984) and the expression of von Willebrand Factor as a marker of endothelial cells were determined. The population of acetyl LDL positive cells (Fig. 1c; upper and lower parts) and von Willebrand Factor positive cells (Fig. 1d; upper and lower parts) derived from $AC133^+$ cells was 5–6 times higher than those of $CD34^+$ cells ($P < 0.05$ and < 0.001, respectively). Since these results suggest that $AC133^+$ cells include many more endothelial progenitor cells than $CD34^+$ cells, the following experiments were performed using $AC133^+$ cells.

We examined the differentiation ability of $AC133^+$ cells in terms of several endothelial markers. As shown in Figure 2, after 2 weeks of culture, adherent cells from $AC133^+$ cells expressed CD31 (PECAM-1), Tei2, KDR (Flk-1) and eNOS. In particular, fibroblastic cells were strongly stained with endothelial Tei2 and KDR antibodies, while eNOS was also observed in round-shaped

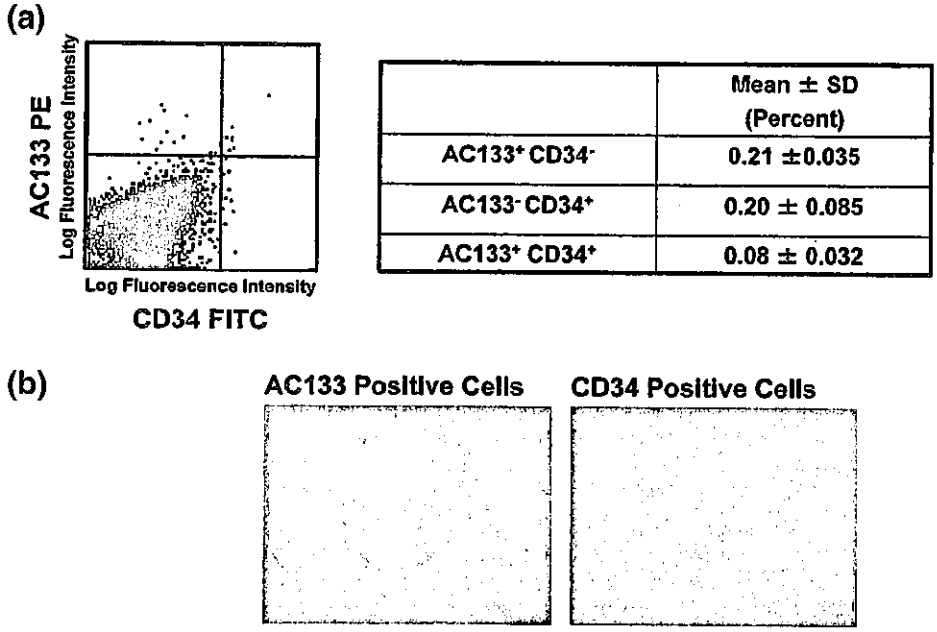

	Mean ± SD (Percent)
$AC133^+$ $CD34^-$	0.21 ±0.035
$AC133^-$ $CD34^+$	0.20 ± 0.085
$AC133^+$ $CD34^+$	0.08 ± 0.032

Fig. 1. In vitro differentiation of $AC133^+$ cells and $CD34^+$ cells into endothelial cells. Both $AC133^+$ cells and $CD34^+$ cells were cultured for 2 weeks in the presence of VEGF on FN-coated dishes. Two weeks after the inoculation, adherent cells were fixed and then subjected into microscopic and immunofluorescence observation. **a**: AC133 and CD34 expression in human peripheral blood mononuclear cells was revealed by staining with AC133-PE (vertical axis) and CD34-FITC (horizontal axis). The lines indicate the border of each positive and negative population. The right-side table shows the mean ± SD (n = 3) of the percentage in each population. **b**: Phase-contrast microscopic photograph of differentiated $AC133^+$ and $CD34^+$ cells. Acetyl-LDL incorporation (**c**) and expression of von Willebrand factor (**d**) were examined as described in "Materials and Methods." The left part show the fluorescent photomicrographs and the right part show the photomicrographs of the same area. Scale bar, 100 μm. Columns and bars represent the means ± SD of acetyl-LDL positive cells or von Willebrand factor positive cells of three fluorescent photomicrographs ($^*P < 0.05$; $^{***}P < 0.001$). [Color figure can be viewed in the online issue available at www.interscience.wiley.com.]

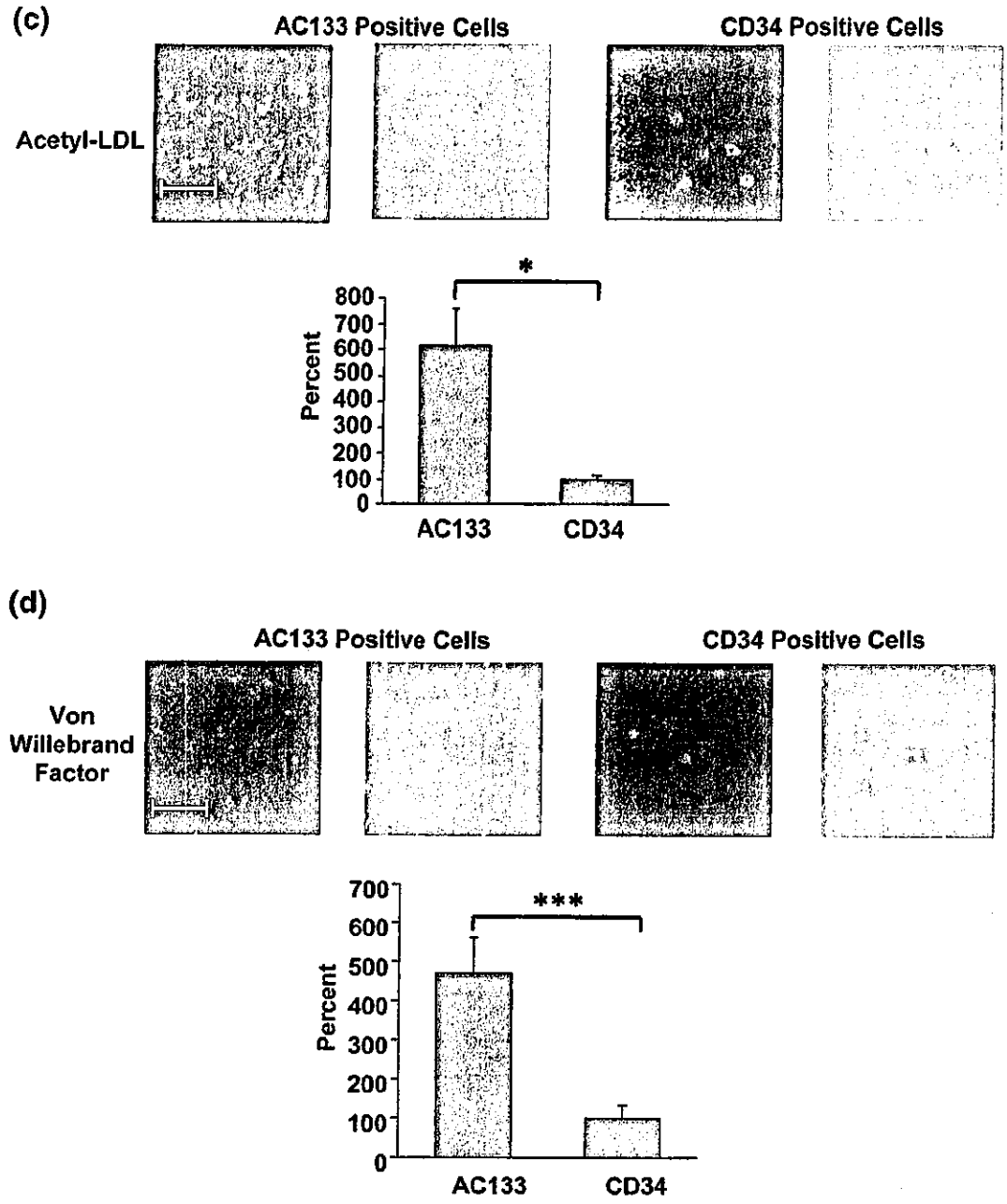

Fig. 1. (*Continued*)

cells. The chronological expression of endothelial marker on AC133$^+$ cells is shown in Figure 3. One week after the inoculation of AC133$^+$, many cells became adherent to the FN-coated dish but scarcely extended on the dish. Two weeks after the inoculation, the adherent cells began to extend, and two-types of cells, such as fibroblast-like cells and more round-shaped cells, appeared. The significant CD31 expression was observed a week after the inoculation and gradually decreased as a function of the time elapsed. By the quantitative analysis of the fluorescence intensity, the expression of CD31 at 1 week was about five times higher than that at 2 weeks (Fig. 3a, $P < 0.001$). On the other hand, the expression of KDR on cultured AC133$^+$ cells reached its maximum at 2 weeks after the inoculation, and was about three times higher than that at 1 week (Fig. 3b). Although KDR expression was weak at 3 weeks, cells were stained with vWF and had the ability to incorporate acetyl-LDL (data not shown). The expression of eNOS was constant (Fig. 3c) but CD11b as a myeloid cell marker was scarcely detected on cultured AC133$^+$ cells during 3 weeks incubation (Fig. 3d). These results

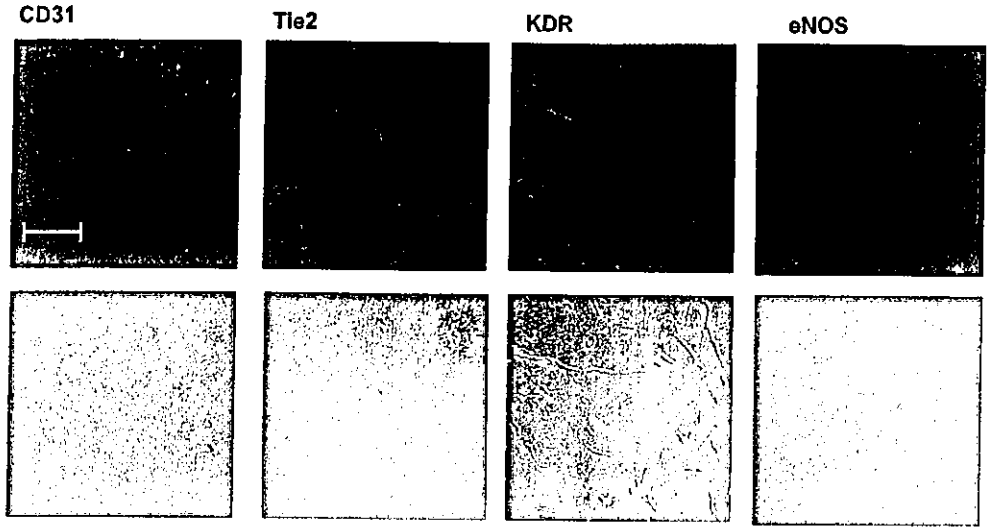

Fig. 2. CD31, Tie2, KDR, and eNOS expression on differentiated AC133+ cells. AC133+ cells were cultured for 2 weeks in the presence of VEGF on FN-coated dishes. Cultured cells were stained with specific antibodies followed by FITC-labeled (for CD31, Tie2, and KDR) or Rhodamin-labeled second antibodies. The upper part shows the fluorescent photomicrographs and the lower part show the photomicrographs of the same area. Scale bar, 100 μm.

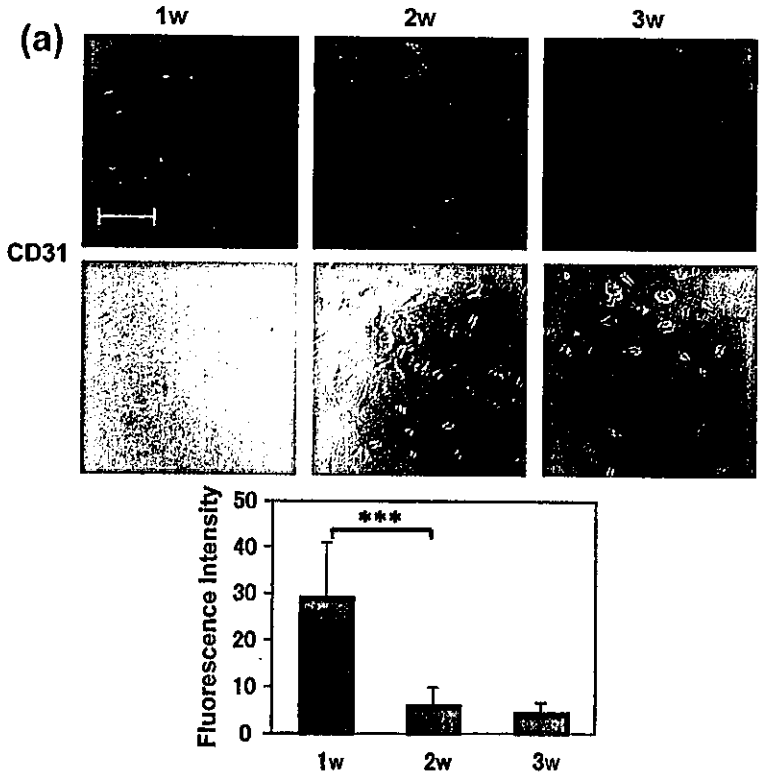

Fig. 3. Chronological expression of endothelial marker on cultured AC133+ cells. AC133+ cells were differentiated in the presence of VEGF on FN-coated dishes. One week, two weeks, and three weeks after the inoculation, the cells were fixed with absolute ethanol. After being washed with PBS, the expression of each endothelial marker was examined as described in Figure 2. CD11b expression was examined with anti-CD11b antibody followed by FITC-labeled second antibody. The upper part shows the fluorescent photomicrographs and the lower part shows the photomicrographs of the same area; (a) CD31, (b) KDR, (c) eNOS, (d) CD11b. Scale bar, 100 μm. Quantitation of fluorescence intensity of 20 cells was performed as described in "Materials and Methods." Columns and bars represent the means ± SD of each cell. (***$P < 0.001$).

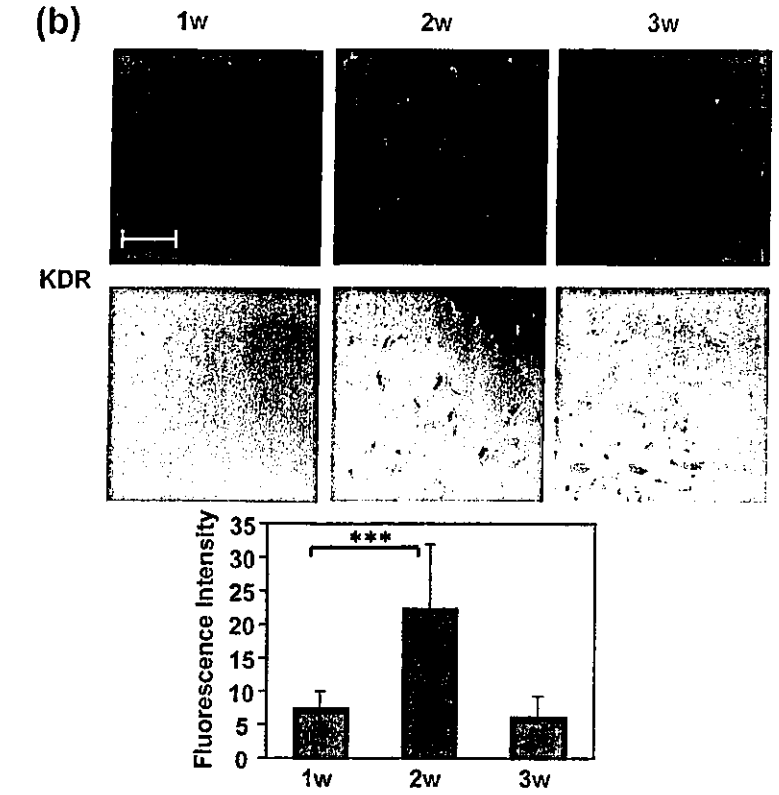

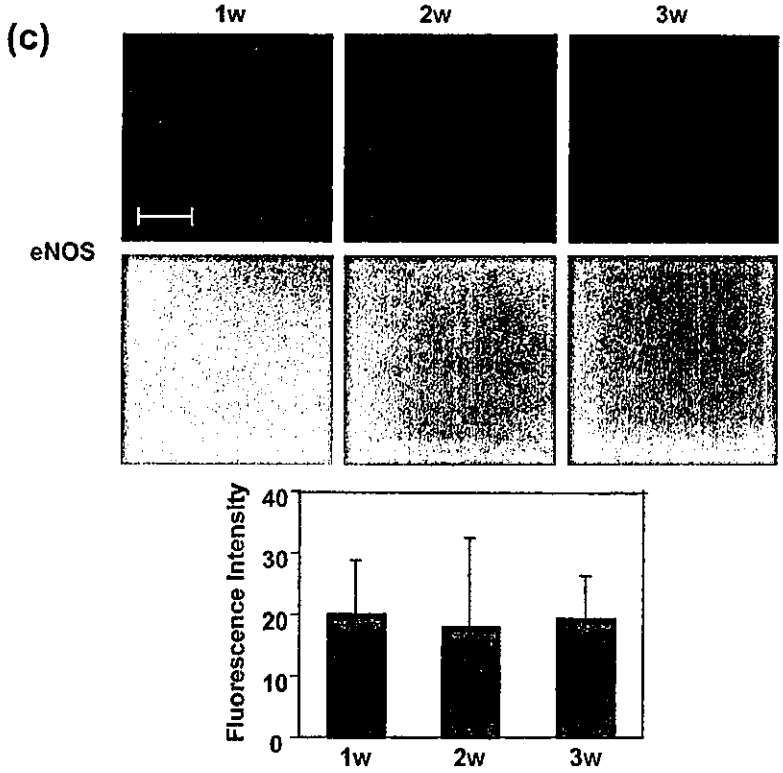

Fig. 3. (*Continued*)

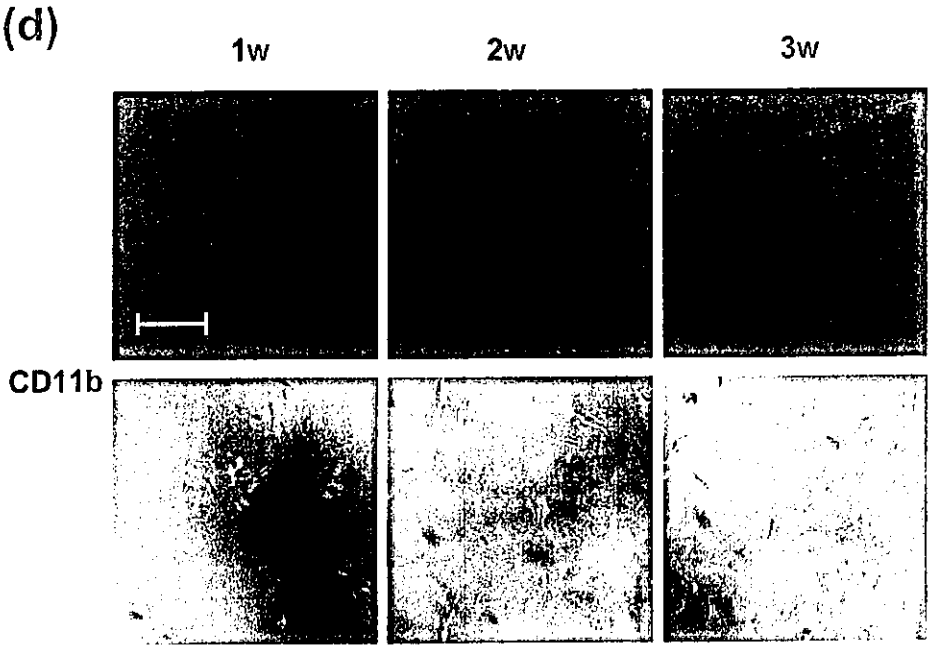

Fig. 3. (*Continued*)

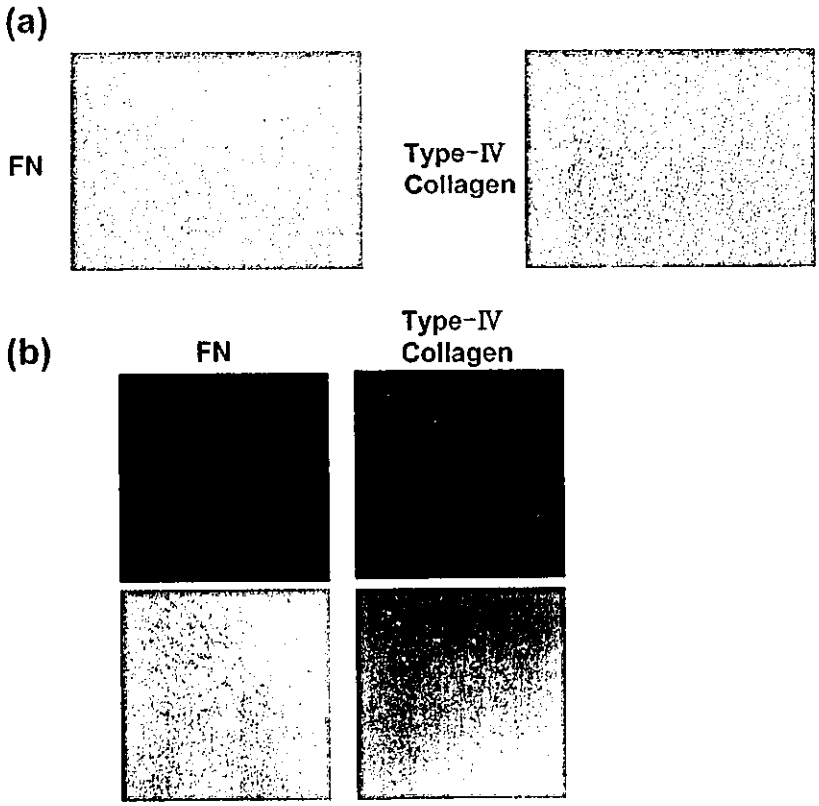

Fig. 4. Effect of the extracellular matrix on the differentiation of AC133+ cells. AC133+ cells were differentiated for 1 week in the presence of VEGF on FN- or collagen type IV-coated dishes. **a**: Unfixed cells were observed under phase-contrast microscopy. **b**: CD31 expression was examined as described in Figure 2. The upper part shows the fluorescent photomicrographs and the lower part shows the photomicrographs of the same area.

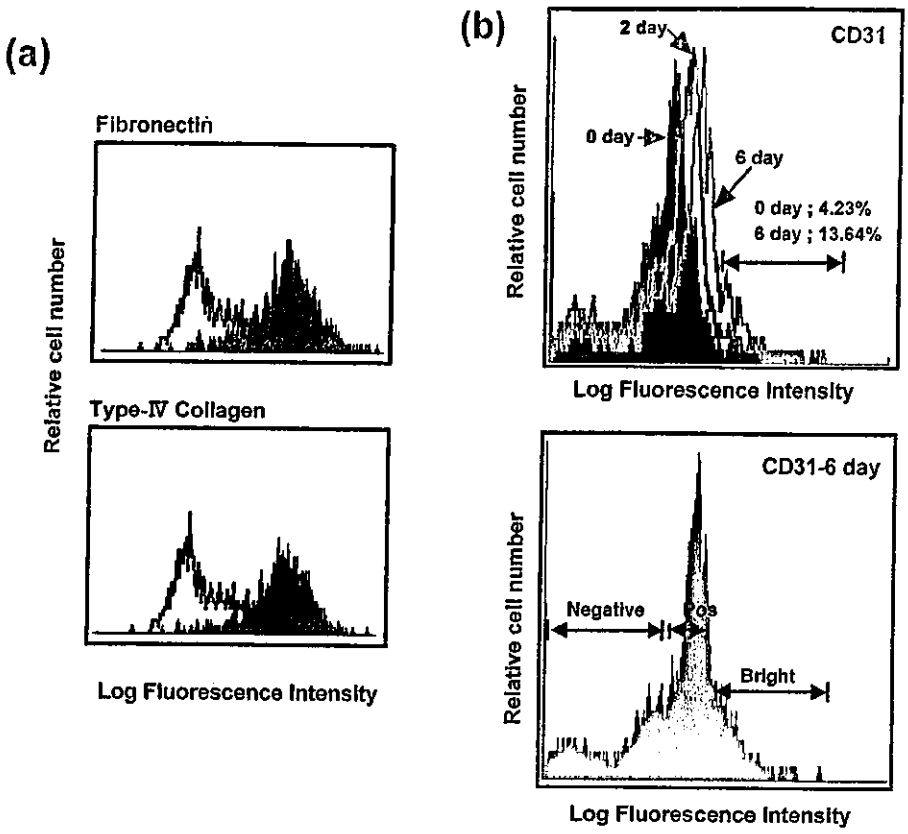
(a)
Fibronectin
Relative cell number
Type-IV Collagen
Log Fluorescence Intensity
(b)
2 day
CD31
0 day
6 day
0 day ; 4.23%
6 day ; 13.64%
Relative cell number
Log Fluorescence Intensity
CD31-6 day
Negative
Pos
Bright
Relative cell number
Log Fluorescence Intensity

Fig. 5.

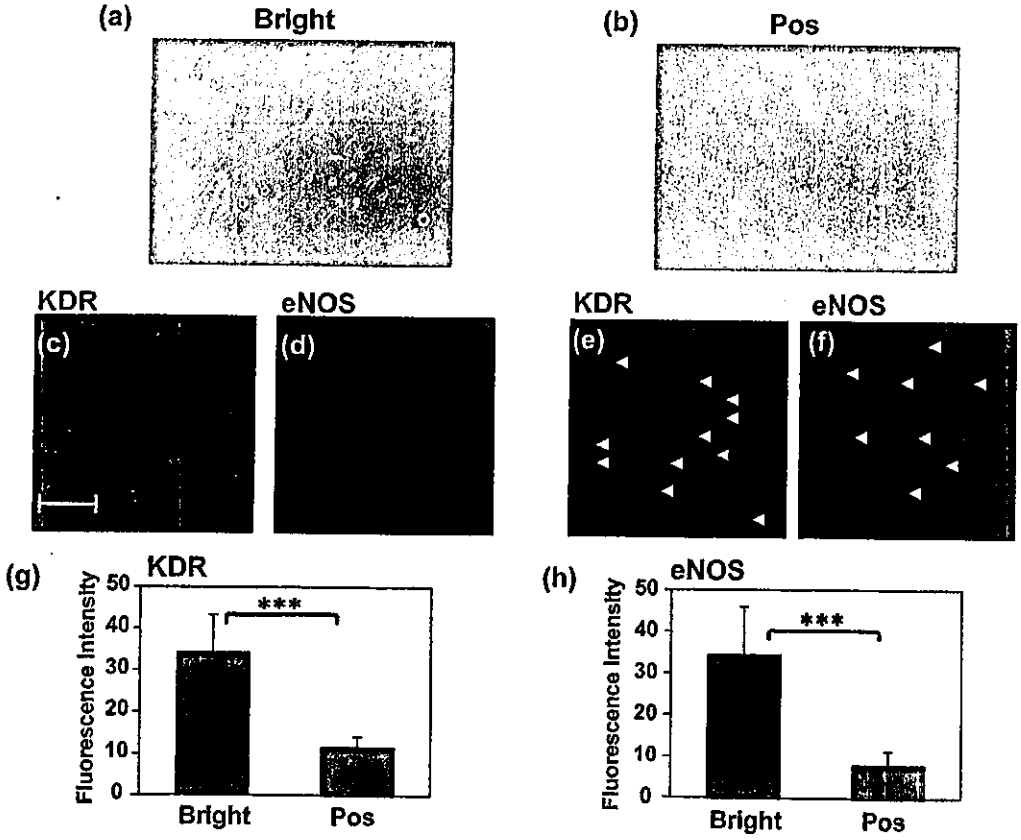
(a)
Bright
(b)
Pos
KDR
(c)
eNOS
(d)
KDR
(e)
eNOS
(f)
(g)
KDR
Fluorescence Intensity
50
40
30
20
10
0
***
Bright
Pos
(h)
eNOS
Fluorescence Intensity
50
40
30
20
10
0
***
Bright
Pos

Fig. 6.

suggest that the expression of CD31 is the earliest event during the differentiation of endothelial cells from AC133$^+$ cells.

Recently, Yamashita et al. (2000) reported that endothelial cells arise from KDR-expressing mesoderm cells, which were derived from mouse ES cells cultured for four days on collagen IV-coated dishes. This observation suggests that the extracellular matrix plays an important role in the differentiation of embryonic endothelial progenitor cells. We therefore compared the differentiation of adult peripheral blood AC133$^+$ cells into endothelial cells when cultured on various extracellular matrix-coated dishes. As shown in Figure 4a, when AC133$^+$ cells were cultured for a week on either FN-coated or type IV collagen- coated dishes, a few adherent cells and many non-adherent cells were observed. The adherent cells that were cultured on type IV collagen-coated dishes for a week scarcely extended on the dish as compared with cells cultured on FN-coated dishes (Fig. 4a). However, when both adherent and non-adherent cells cultured on type IV collagen-coated dishes for one week were collected and cultured for 2 subsequent weeks on FN-coated dishes, but not on type IV collagen-coated dishes, these cells exhibited the same endothelial markers as cells cultured on only FN-coated dishes for 3 weeks (data not shown). As shown in Figure 4b, there was no difference of the expression of CD31 for 1 week between FN and type IV collagen-coated dishes. These findings suggest that 1 week of incubation, the early differentiation of AC133$^+$ cells into endothelial cells is not affected by the difference between FN-coated or type IV collagen-coated dishes, but the interaction of the cells with FN might be required for further differentiation.

The above results indicated that the expression of CD31 may be an observable early indicator of endothelial differentiation. To assess the relationship between CD31 expression and the ability to differentiate into endothelial cells in cultured AC133$^+$ cells, we sorted cultured AC133$^+$ cells in terms of CD31 expression. As shown in Figure 5a, there was no difference in CD31 expression in AC133$^+$ cells between those cultured on type IV collagen-coated dishes and those cultured on FN-coated dishes. The following experiments were performed using AC133$^+$ cells cultured on type IV collagen-coated dishes because of the greater feasibility of cell collection. The expression of CD31 on AC133$^+$ cells gradually increased during 1 week of culture, and CD31-brightly expressed cells appeared as the culture proceeded (Fig. 5b; upper part). The percentage of the CD31-brightest fraction indicating by arrow increased from 4.23–13.64% during 6 days (Fig. 5b; upper part).

Next, we sorted CD31-bright cells, CD-31 positive cells, and CD-31 negative cells (Fig. 5b; lower part) from AC133$^+$ cells cultured for 6 days on type IV collagen-coated dishes. To examine these cells' ability for endothelial differentiation, the sorted cells were cultured for one subsequent week on FN-coated dishes. As shown in Figure 6, many more adherent cells appeared from CD31-bright cells (a) than from CD31-positive cells (b), and no adherent cells appeared from CD31-negative cells. When the expressions of KDR (Fig. 6c,e,g) and eNOS (Fig. 6d,f,h) in CD31-bright and -positive cells were analyzed, the adherent cells derived from CD31-bright cells were found to show markedly higher expression of eNOS and KDR than that in those derived from CD31-positive cells, suggesting that CD31-bright cells have an ability to differentiate into endothelial cells. On the other hand, the adherent cells in the CD31-positive population may be monocytes/macrophages.

DISCUSSION

Several studies indicated that not only bone-marrow cells but also adult peripheral blood cells contain endothelial progenitor cells. Peichev et al. (2000) suggested that circulating CD34$^+$ cells expressing VEGFR-2 and AC133 constitute a phenotypically and functionally distinct population of circulating endothelial cells that may play a role in neo-angiogenesis. AC133$^+$ cells in bone-marrow also have been reported to be endothelial progenitor cells (Gehling et al., 2000; Quirici et al., 2001). Endothelial progenitor cells in both bone-marrow and cord-blood have been reported to express CD34$^+$ on the cell surface (Nieda et al., 1997; Gaugler et al., 2001; Quirici et al., 2001). In the present study, we compared the endothelial differentiation abilities of AC133$^+$ cells and CD34$^+$ cells isolated from peripheral blood mononuclear cells. Whereas Yin et al. (1997) suggested that AC133$^+$ cells were a subset of CD34$^+$ cells, we observed AC133$^+$ CD34$^-$ in the peripheral blood mononuclear cells (Fig. 1a). The differentiated cells from the AC133$^+$ cells expressed many more endothelial markers than did those from CD34$^+$ cells (Fig. 1c,d). Therefore, we concluded that AC133$^+$ cells isolated from human peripheral blood mononuclear cells are better able to differentiate into endothelial cells than are CD34$^+$ cells. Reyes et al. (2002) reported that the origins of endothelial progenitors

Fig. 5. Flow cytometric analysis of CD31 expression on cultured AC133$^+$ cells. AC133$^+$ cells were differentiated in the presence of VEGF on FN- or collagen type IV-coated dishes for 6 days. **a**: Comparison of CD31 expression on AC133$^+$ cells cultured between FN- and collagen type IV-coated dishes. **b**: Time-dependent alteration of CD31 expression on cultured AC133$^+$ cells on collagen type IV-coated dishes.

Fig. 6. Endothelial differentiation of CD31-bright and CD31-positive cells. Six days after the inoculation, AC133$^+$ cells were sorted into CD31-bright, CD31-positive, and CD31-negative cells as shown in Figure 5b. After the sorting, the cells were subsequently cultured with VEGF on FN-coated dishes for 1 week. **a**: Photograph of differentiated CD31-bright cells. **b**: Photograph of differentiated CD31-positive cells. **c** and **e**: Differentiated CD31-bright and -positive cells were stained with anti-KDR antibody followed by staining with FITC-labeled second antibody, respectively. **d** and **f**: Differentiated CD31-bright and -positive cells were stained with anti-eNOS antibody followed by staining with Rhodamin-labeled second antibody, respectively. Because of the low fluorescence intensity of both markers in cultured CD31-positive cells, arrowheads are used to indicate the presence of adherent cells. Scale bar, 100 μm. **g** and **h**: Quantitation of fluorescence intensity of KDR and eNOS in cultured CD31-bright and -positive cells was performed as described in "Materials and Methods." Columns and bars represent the means ± SD of each cell. (***$P < 0.001$).